Proceedings of the ASME 2010 3rd Joint US-European Fluids Engineering Summer Meeting and 8th International Conference on Nanochannels, Microchannels, and Minichannels
FEDSM-ICNMM2010
August 1-5, 2010, Montreal, Canada

FEDSM-ICNMM2010-30788

A NEW PROCEDURE TO CAPTURE TEMPERATURE FLUCTUATIONS USING COLD WIRES: APPLICATION TO THERMOACOUSTIC SYSTEMS

Arganthaël Berson
Fuel Cell Research Centre
Queen's University
Kingston, Ontario, Canada

Gaëlle Poignand
LMFA UMR CNRS 5509
Ecole Centrale de Lyon
Ecully, France

Philippe Blanc-Benon
LMFA UMR CNRS 5509
Ecole Centrale de Lyon
Ecully, France

Geneviève Comte-Bellot
LMFA UMR CNRS 5509
Ecole Centrale de Lyon
Ecully, France

ABSTRACT

The improvement of the thermal coupling between the stack of a thermoacoustic refrigerator and the heat exchangers is necessary to achieve high-efficiency and stable operation. Heat transport by the thermoacoustic effect depends on both the velocity and temperature fields. Inside the stack, it can be described by the linear theory of thermoacoustics. However, departures from linear behaviours are expected near the edges of the stack and in the heat-exchangers due to the generation of vorticity and temperature harmonics. The present work focuses on the experimental characterization of temperature harmonics near the edges of a thermoacoustic stack. Experiments are conducted in an 18cm-long resonator operated with air at atmospheric pressure at the resonance frequency of approximately 464Hz. Drive ratios up to 3% are achieved, which corresponds to temperature oscillation amplitudes up to 2.5K. Temperature measurements are performed using a novel procedure recently proposed by Berson et al., Rev. Sci. Instrum. 81, 015102 (2010). The instantaneous temperature is measured with a cold wire operated by a Constant-Current Anemometer (CCA). In addition, we record the output signal of the same wire, under the same flow conditions – which is made possible by the periodicity of the acoustic wave – and operated in the heated mode by a Constant-Voltage Anemometer (CVA). During post-processing, the thermal inertia of the cold wire operated with the CCA is corrected using the CVA signal. This procedure does not require any physical properties of the wire such as the diameter. In addition, it does not require the knowledge of a heat-transfer/velocity relationship for the wire. This is all the most important for thermoacoustic systems since no such relationship is available in oscillating flows. Results validate the generation of temperature harmonics near the stack edges. The spatial distributions of the first and second harmonic amplitudes are compared with a one-dimensional model. The model is an extension of an analytical model from the literature [Gusev et al., J. of Sound and Vibration 235, (2000)] that takes into account axial conduction. Experimental results show an excellent qualitative agreement with the model and demonstrate the importance of axial conduction on the nonlinear thermal field behind the stack.

NOMENCLATURE

c_p specific heat of the fluid
c_w specific heat of the wire material
d_{ac} acoustic displacement

D diffusivity of the fluid
d_w wire diameter
f_{osc} fundamental frequency of acoustic oscillations
l_w wire length
m_w mass of the wire
$\mathscr{M}_{CCA}$ time lag of the cold wire
P' pressure fluctuations
Pe^{-1} inverse of the Péclet number
R relaxation coefficient
R_{CCA} resistance of the real wire
R^*_{CCA} resistance of the ideal wire
R_0 cold resistance of the wire
r_L resistance of the connection cable
t time
T_a temperature of the fluid
T_0 reference temperature
T_m mean temperature of the fluid
T' temperature fluctuations
U velocity component normal to the wire
u' velocity fluctuations
V_w voltage across the wire
x axial coordinate starting from the loudspeaker
$\tilde{x}$ axial coordinate starting from the closed end of the resonator
y, z transverse spatial coordinates
β thermal expansion coefficient of the fluid
θ normalized temperature fluctuations
θ_1 normalized amplitude of temperature fluctuations at f_{osc}
θ_2 normalized amplitude of temperature fluctuations at $2f_{osc}$
ξ normalized position
ρ_f fluid density
ρ_w density of the wire material
τ normalized time
τ_R relaxation time
χ temperature coefficient of resistivity for the wire material
ω angular frequency

INTRODUCTION

Thermoacoustic systems convert thermal energy into acoustic energy and vice-versa. In thermoacoustic refrigerators, the interaction between a high-amplitude acoustic wave and a porous medium (usually referred to as "stack") creates a heat flux along the porous medium. Thermoacoustic coolers have a simple architecture with no moving part save for the driver, which makes them robust, reliable and opens possibilities for low cost production and miniaturization. In order to improve the performances of such systems, it is necessary to improve the efficiency of each of their components as well as the coupling between these components. The problem of the coupling between the stack and the heat-exchangers has been addressed recently numerically [1–3], analytically [4–7] and experimentally [8], although the latter study adresses aerodynamics only. Analytical models developed by Gusev et al. [4, 5] and later extended by [6, 7] show that the thermal field near the edge of the stack is nonlinear. Thermal harmonics are generated near the end of the stack that affect the transport of heat towards the heat-exchangers. Contrary to the results of the linear theory, these nonlinear models predict that the enthalpy flux towards the heat exchanger is maximised when an optimal gap is introduced between the two components. These results were confirmed by numerical simulations [1–3] but, to date, there is no experimental evidence of the nonlinearity of the temperature field near the stack ends. The objective of this paper is to provide such evidence.

First, we present a one-dimensional model that describes the acoustic temperature field behind the stack. The model is an extension of the work by Gusev et al. [4, 5] that accounts for axial conduction. Indeed, we shall see that axial conduction has a significant effect on the results. Second, we describe how the measurements of temperature fluctuations behind the stack are performed. We use a novel procedure that we developed recently for the measurements of temperature fluctuations in oscillating flows using cold wires [9]. The procedure relies on the unique features of constant-voltage anemometers (CVA) that allows to correct the thermal inertia of cold wires. Eventually, the experimental results are compared with the model predictions.

Model

The problem is similar to the one addressed by Gusev et al. [4]. Inside a thermoacoustic standing-wave refrigerator, the temperature fluctuations inside the channels of the stack are given by the following energy equation:

$$\frac{\partial T'}{\partial t}+u'\frac{\partial T'}{\partial x}=\frac{\beta T_m}{\rho_f c_p}\left(\frac{\partial P'}{\partial t}+u'\frac{\partial P'}{\partial x}\right)+D\left(\frac{\partial^2 T'}{\partial x^2}+\frac{\partial^2 T'}{\partial y^2}+\frac{\partial^2 T'}{\partial z^2}\right) \tag{1}$$

where the different notations are given in the nomenclature. In order to obtain Eq.1, we neglect the effect of viscous stress on the temperature field. Therefore, the flow is one-dimensional and the model does not account for the vortices that appear behind the stack edges [8, 10–14]. We also neglect the thermal dependency of the thermophysical properties of the fluid and solid. However, contrary to Gusev et al. [4], we do not neglect axial conduction. Transverse heat transfer averaged over the channel cross section is modeled by

$$D\iint_S\left(\frac{\partial^2 T'}{\partial y^2}+\frac{\partial^2 T'}{\partial z^2}\right)=D\oint_\Pi\frac{h}{k_f}(T'-T'_s)d\Pi, \tag{2}$$

where S and Π are the surface area and perimeter of a channel cross section, respectively. h is the heat transfer coefficient

and k_f is the conductivity of the fluid. T_s' are the temperature fluctuations of the channel walls, which we neglect. Therefore, we can introduce the relaxation time τ_R

$$\tau_R = \frac{Sk_f}{\Pi dh}. \tag{3}$$

Observing that the second term of the right-hand side of Eq.1 is small compared to the first term, temperature fluctuations averaged over the channel cross section S are given by:

$$\frac{\partial \overline{T'}}{\partial t} + u' \frac{\partial \overline{T'}}{\partial x} = \frac{\beta T_m}{\rho_f c_p} \frac{\partial \overline{P'}}{\partial t} - \frac{\overline{T'}}{\tau_R} + D \frac{\partial^2 \overline{T'}}{\partial x^2}, \tag{4}$$

Eventually, Eq.4 is made nondimensional in a similar way as in [4], which yields:

$$\frac{\partial \theta}{\partial \tau} + \sin\tau \frac{\partial \theta}{\partial \xi} = \sin\tau - \frac{\theta}{R} + Pe^{-1} \frac{\partial^2 \theta}{\partial \xi^2}. \tag{5}$$

where θ represents the temperature fluctuations normalized by the adiabatic temperature fluctuations due to the acoustic wave only, ξ is the distance normalized by the acoustic displacement, τ is the time normalized by the acoustic fundamental frequency, $R = \omega\tau_R$, and $Pe^{-1} = D/(\omega d_{ac}^2)$ is the inverse of the Péclet number based on the acoustic displacement and the acoustic velocity.

Because of the addition of axial conduction, Eq.5 can no longer be solved analytically. Therefore, we use a finite-difference scheme in both time and space in order to obtain a numerical solution for Eq.5. The computational domain ranges from $\xi = -4$ to $\xi = 11$. The stack is located at $\xi \leq 0$. Note that it is not possible to measure the coefficient R so that we arbitrarily set $R = 1$, which is the optimal regime for thermoacoustic performances [4]. For $\xi > 0$, the fluid is only subject to the acoustic wave and does not exchange temperature with its surroundings so that the regime is adiabatic and we set $R = 10000 \approx \infty$.

Measurements of temperature fluctuations behind the stack

Experimental setup

The experimental setup is presented in Figure 1. The thermoacoustic system consists of a quarter-wavelength standing-wave acoustic resonator, a stack of plates and sensors. The resonator is a 15-cm long straight cylindrical tube of diameter 3cm. A 3-cm long exponential horn connects one end of the tube to the electrodynamic driver (GELEC EDM8760F). The other end is closed. The driver generates acoustic pressure levels up to 3000Pa at the fundamental frequency of $f_{osc} = 464$Hz in air at ambient temperature and atmospheric pressure. The acoustic pressure is monitored by a $1/4$ in. Bruel & Kjaer microphone located at $\tilde{x} = 90$mm from the closed end of the resonator.

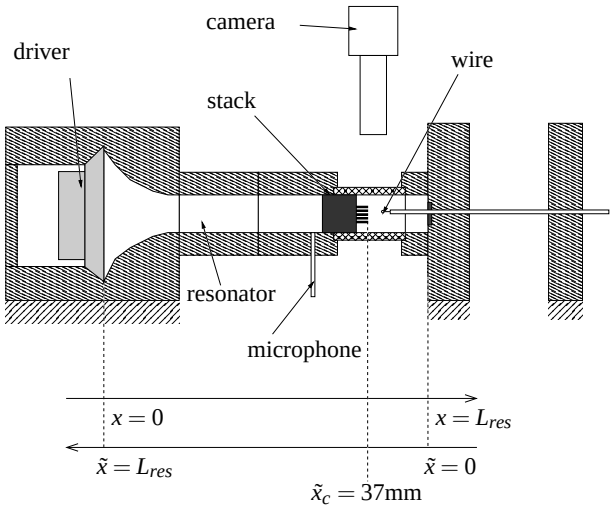

FIGURE 1. Experimental setup.

The stack is made of parallel glass plates of thickness $e_0 = 0.17$mm, of length $l = 18$mm and separated by $2y_0 = 0.41$mm. The total blockage ratio of the stack, including the support is $BR = 0.39$. The hot side of the stack is located $\tilde{x}_c = 37$mm away from the closed end of the resonator. In this configuration, a temperature gradient of approximately $9K$ develops along the stack at $P_{ac} = 3000$Pa.

Temperature measurements are performed with a small tungsten wire. The diameter of the wire is approximately 3μm and its length is 3mm. The wire is mounted on a L-shaped probe (Dantec 55P04). It is very important that the wire be mounted on such a L-shaped probe in order to avoid interactions between the fluid and the wire support during an acoustic cycle [6]. The cold resistance of the wire is $R_0 = 24.9\Omega$ and the resistance of the connection cable is $r_L = 0.7\Omega$. The wire is inserted in the resonator through a rubber membrane embedded in the end wall, which ensures an adequate sealing. The distance between the wire and the stack plates along the resonator axis is controlled with an accurate linear stage and monitored with a camera equipped with a zoom lens. The wire is set parallel to the stack plates and in front of the shear layers developing along the plate surface.

Procedure for temperature measurements in oscillating flows using cold wires

For the measurements of temperature fluctuations behind the stack, we follow the procedure we previously developed and val-

idated in [9]. To our knowledge, this is the only procedure available that allows the accurate measurements of temperature fluctuations in oscillating flows using cold wires. In the following, we briefly summarize this procedure. More details can be found in [9].

When operated in the constant-current mode (CCA) with a very low overheat, the resistance of the thin metallic wire described in the previous section varies with the temperature of the surrounding fluid:

$$T_a(t) - T_0 = \frac{R^*_{CCA}(t) - R_0}{R_0 \chi}, \tag{6}$$

where $R^*_{CCA}(t)$ is the resistance of an ideal wire, i.e. a wire without thermal inertia. Indeed, the wire resistance does not respond instantaneously to a change in the fluid temperature. The resistance $R_{CCA}(t)$ of the real wire is related to the resistance of the ideal wire by the following equation

$$\mathscr{M}_{CCA}(t) \frac{dR_{CCA}(t)}{dt} + R_{CCA}(t) = R^*_{CCA}(t), \tag{7}$$

where $\mathscr{M}_{CCA}(t)$ is the time lag of the cold wire, which is given by:

$$\mathscr{M}_{CCA}(t) = \frac{m_w c_w}{\chi R_0} \frac{1}{f[U(t)]}. \tag{8}$$

$\mathscr{M}_{CCA}(t)$ can be separated into two terms. The first one $m_w c_w / \chi R_0$ depends on the wire properties and the second one is a function of the flow velocity $1/f[U(t)]$.

The first term of the time lag, $m_w c_w / \chi R_0$, is straightforwardly obtained by using the square-wave test circuit embedded in the CVA units from Tao Systems [15,16]. The procedure is described in more details in [9,17]. Note that it does not require to know the thermophysical and geometrical properties of the wire, which is very convenient since the wire diameter for instance always differs from the specifications of the manufacturer.

The second term of the time lag, $1/f[U(t)]$, depends on the flow velocity and, hence, it is time dependent. If $\mathscr{M}_{CCA}(t)$ fluctuates, the wire no longer behaves as a first-order system. This is the case in an oscillating flow. It becomes nonlinear and Eq.7 generates higher harmonics in the measured signal $R_{CCA}(t)$ that are not present in the excitation signal $R^*_{CCA}(t)$ [18]. Therefore it is necessary to measure accurately $1/f[U(t)]$. To do so, the same wire is operated in the heated mode so that it becomes sensitive to the amount of heat convected away from the hot wire by the fluid flow, which usually allows to calculate the instantaneous fluid velocity. In the acoustic wave, because the flow changes direction during an acoustic cycle, no relationship between the convective flux and the velocity is available [6,19]. It is not possible to measure the velocity but we demonstrated that the CVA gives $f[U(t)]$ directly [9,17]. The procedure does not require any calibration in velocity and, in addition, it corrects for all the nonlinearities of the CVA in the hot-wire mode.

We perform measurements in the cold-wire and hot-wire modes alternately, the measurements being synchronized with the output signal of the monitoring microphone. Cold-wire measurements are performed with the temperature module of a Dantec Streamline 90C20 anemometer. The intensity of the current flowing through the wire is maintained constant by the anemometer to $I_{CCA} = 0.1$mA. Hot-wire measurements are performed with a CVA, model VC01 from Tao Systems, maintaining a constant voltage $V_w = 910$mV across the wire. More details about the electronics and the parameters of the anemometers are given in [9]. During post-processing, Eq.7 is solved numerically using $\mathscr{M}_{CCA}(t)$ that is computed from CVA measurements, and the instantaneous temperature of the fluid is deduced from the resistance of the ideal wire using Eq.6 or a calibration curve.

Results

Figures 2 and 3 show the spatial distributions of the amplitudes of temperature fluctuations behind the stack at the fundamental frequency and twice the fundamental frequency, respectively. Measurements were performed at three different pressure levels: $P_{ac} = 1000$, 2000 and 3000Pa. The coefficients Pe^{-1} corresponding to these pressure levels are: $Pe^{-1} = 16.3 \times 10^{-3}$,$3.8 \times 10^{-3}$ and 1.9×10^{-3} respectively. They were calculated using $D = 2.2 \times 10^{-5}\text{m}^2.\text{s}^{-1}$ as the diffusivity coefficient of air. We also plotted the results obtained with the analytical model by Gusev et al. [4], which corresponds to the case $Pe^{-1} = 0$ (no conduction), as a reference.

We first look at the results from the model, in order to assess the effect of axial conduction on the thermal field behind the stack. Harmonics are generated due to the change in transverse-heat-transfer regime between the two regions of the domain. The analytical model, in which axial conduction is neglected, predicts that the thermal field is nonlinear up to $\xi = 2$ away from the stack edge. Indeed, a fluid particle driven by the acoustic wave oscillates with an amplitude of $2d_{ac}$. As we can see on Fig. 4, only the fluid particles with their rightmost position located closer than $2d_{ac}$ from the stack end interact with the stack plates so that locations for $\xi \geq 2$ are never "visited" by a particle that interacts with the stack. Adding axial conduction to the model extends the size of the perturbated region behind the stack beyond $\xi = 2$. The greater the coefficient Pe^{-1}, the further the perturbated region extends.

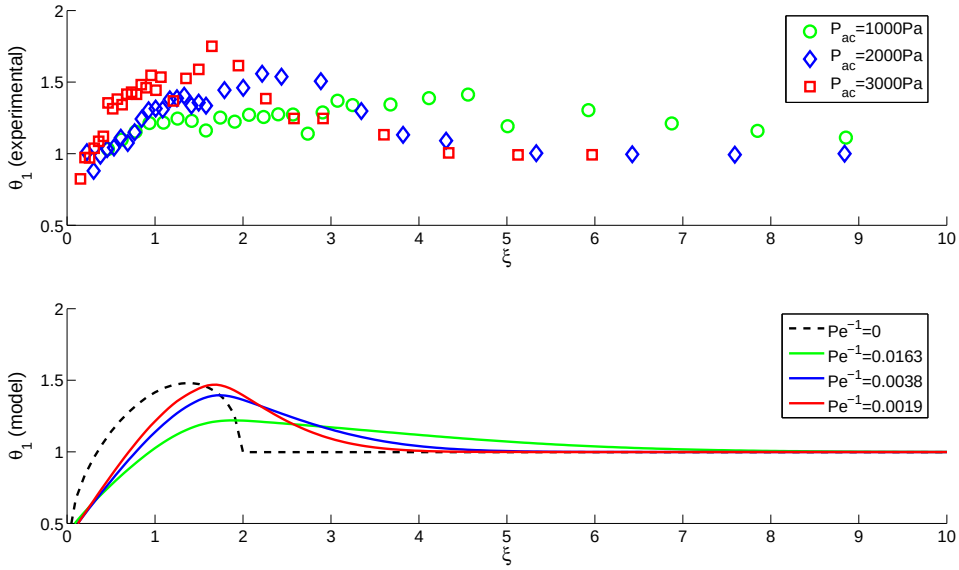

FIGURE 2. Amplitudes of temperature fluctuations behind the stack at the fundamental frequency. Top: measurements. Bottom: model. Relaxation parameter in the stack used in the model $R = 1$. The stack end is located at $\xi = 0$.

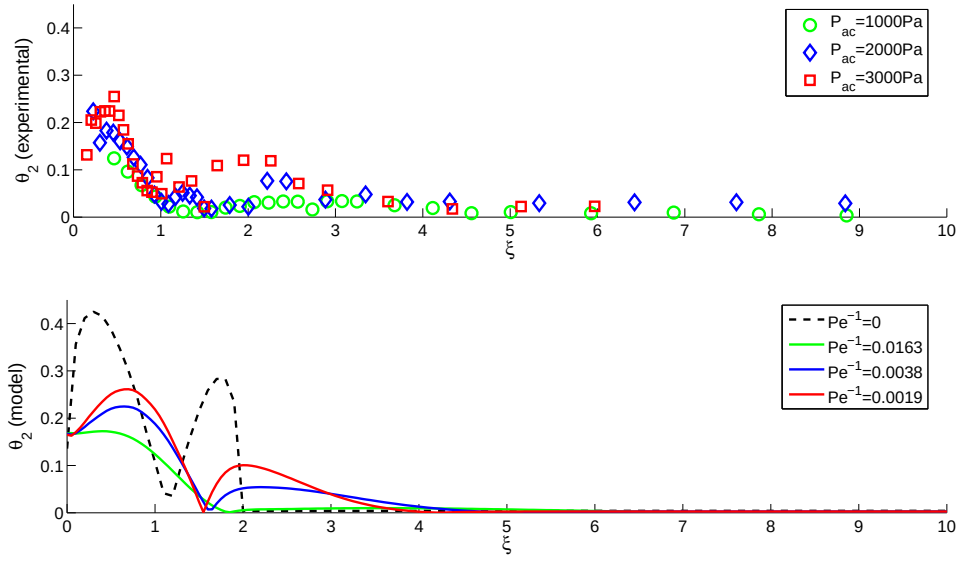

FIGURE 3. Amplitudes of temperature fluctuations behind the stack at twice the fundamental frequency. Top: measurements. Bottom: model. Relaxation parameter in the stack used in the model $R = 1$. The stack end is located at $\xi = 0$.

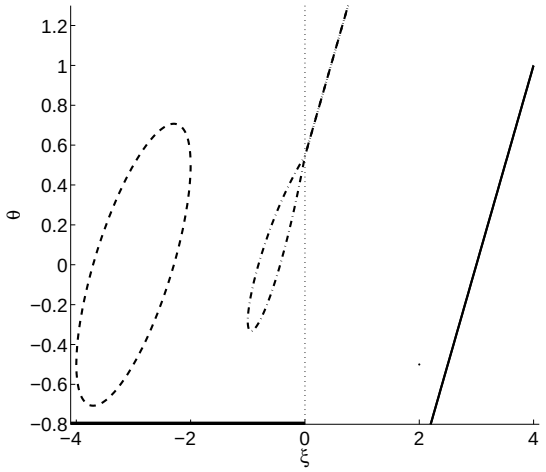

FIGURE 4. Position and temperature of three fluid particles during an acoustic cycle. The leftmost particle spends the entire acoustic cycle inside the stack ($R = 1$). The rightmost particle spends the entire acoustic cycle outside the stack ($R = \infty$). The middle particle crosses the edge of the stack. Axial conduction is neglected, $Pe^{-1} = 0$.

The analytical model shows that θ_1 reaches a maximum at about $\xi = 1.4$ before going down to $\theta_1 = 1$ at $\xi = 2$ (Figure 2, bottom). Axial conduction shifts the position of the maximum away from the stack and, as already mentioned, extends the zone where $\theta_1 > 1$ beyond $\xi = 2$. The maximum also decreases as Pe^{-1} increases, which flattens the spatial distribution.

The effect of axial conduction on θ_2 is similar. According to the analytical model, there are two maxima of θ_2 behind the stack located at approximately $\xi = 0.3$ et $\xi = 1.7$ (Figure 3, bottom). The first peak is larger than the second one. Again, axial conduction shifts the perturbation away from the stack and beyond $\xi = 2$. Increasing Pe^{-1} decreases the amplitude of both peaks, the second one being more affected. For $Pe^{-1} = 0.0163$, the second peak is hardly distinguishable.

We do not expect our model to compare quantitatively well with the experimental results mostly because the relaxation coefficient, which is a key parameter of the model, is not known and has been chosen arbitrarily. However, we see in Figures 2 and 3 that the measured amplitudes of the peaks for both harmonics are within the same range as the model predictions. More importantly, the qualitative agreement is excellent. The experimental results presented in Figure 2 (top) show the same trend as the model, i.e. a maximum of amplitude is observed, which decreases and is shifted away from the stack when the acoustic pressure decreases. Far from the stack, temperature fluctuations are no longer perturbated and follow an adiabatic cycle ($\theta_1 = 1$). Figure 3 (top) also demonstrates that the measured amplitudes of the second harmonic follow the trends predicted by the model. As the acoustic pressure decreases, i.e. axial conduction becomes more important, the two peaks decrease, the second one being more affected than the first and extending beyond $\xi = 2$.

Conclusion

We have developed a one-dimensional model that captures the nonlinear temperature fluctuations behind the stack of a thermoacoustic refrigerator. Unlike previous studies, the model includes axial conduction, which is seen to affect the temperature profiles significantly. In parallel, we have performed cold-wire measurements of the temperature harmonics generated behind the stack. We have used a procedure recently developed by us, which relies on the unique features of constant-voltage anemometers to correct the thermal inertia of cold wires and is the only way, to our knowledge, to perform accurate temperature measurements in an oscillating flow using cold wires. The experimental results are in excellent qualitative agreement with the measurements.

ACKNOWLEDGMENT

The authors are grateful to Tao Systems, Emmanuel Jondeau and Vitalyi Gusev.

REFERENCES

[1] E. Besnoin, O. Knio, *Acta Acustica united with Acustica* **90**, 432–444 (2004).
[2] D. Marx D. and Ph. Blanc-Benon, *AIAA Journal* **42**(7), 1338–1347 (2004).
[3] D. Marx D. and Ph. Blanc-Benon, *J. Acoust. Soc. Am.* **118**, 2993–2999 (2005).
[4] V. Gusev, P. Lotton, H. Bailliet, S. Job, and M. Bruneau, *J. Acoust. Soc. Am.* **109**, 84–90 (2001).
[5] V. Gusev, P. Lotton, H. Bailliet, S. Job, and M. Bruneau, *J. of Sound and Vibration* **235**, 711–726 (2000).
[6] A. Berson, PhD dissertation (in French), Ch. 3, Ecole Centrale de Lyon, ECL-2007-41 (2007).
[7] A. Berson and Ph. Blanc-Benon, "Nonlinear heat transport between the stack and the heat-exchangers of standing-wave thermoacoustic refrigerators", in Proceedings of the 18th International Symposium on Nonlinear Acoustics, Stockholm, July 7 - 10, 2008, AIP Conf. Proc. 1022, p.359-362 (2008).
[8] A. Berson and Ph. Blanc-Benon, *J. Acoust. Soc. Am.* **122**, EL122–EL127 (2007).
[9] A. Berson, G. Poignand, Ph. Blanc-Benon, G. Comte-Bellot, *Rev. Sci. Instrum.*, **81**, 015102 (2010)
[10] A. Berson, M. Michard, and Ph. Blanc-Benon, *Heat and Mass Transfer*, **44**, 1015–1023 (2007).

[11] P. Aben, P. Bloemen, and J. Zeegers, *Experiments in Fluids*, **46** (4), 631–641 (2009).
[12] L. Shi, Z. Yu, and A.J. Jaworski, *International Journal of Applied Science, Engineering and Technology*, **3** (5), 144–151 (2009).
[13] X. Mao, Z. Yu, A.J. Jaworski, and D.Marx, *Experiments in Fluids*, **45** (5), 833–846 (2008).
[14] X. Mao and A.J. Jaworski, *Measurement Science and Technology*, **21** (3), 035403 (2010).
[15] Sarma G.R., *Rev. Sci. Instrum.*, **69**, 2385-2391, (1998).
[16] Sarma G.R., Lankes R.W., *Rev. Sci. Instrum.*, **70**, 2384-2386 (1999).
[17] A. Berson, Ph. Blanc-Benon and G. Comte-Bellot, *Rev. Sci. Instrum.*, **80**, 045102 (2009).
[18] P. Freymuth, *J. Phys. E: Sci Instrum*, **12**, 351–352 (1979).
[19] T.J. Pedley, *J. Fluid. Mech.*, **67**, 209–225 (1975).